

Gradient Diffusion: Enhancing Existing Neural Models with Homeostatic Control and Tuning

Lennart P. L. Landsmeer^{1,2}, Mario Negrello², Said Hamdioui¹, Christos Strydis^{2,1}

¹Delft Technical University, Department of Quantum and Computer Engineering, Delft, The Netherlands

²Erasmus Medical Center, Department of Neuroscience, NeurocomputingLab, Rotterdam, The Netherlands

December 2024

Abstract

Realistic brain modeling requires precise estimation of numerous unobserved parameters, a task hindered by complex nonlinearities and the inaccessibility of the brain’s full dynamical state. Current multicompartmental-model simulations predominantly rely on gradient-free optimization methods, which suffer from the “curse of dimensionality” and are incompatible with online tuning crucial for emulating biological homeostasis. Gradient-based methods offer superior scalability and facilitate online adaptation but are currently inaccessible within existing brain simulators due to the significant resource investment and incompatibility with established simulators. This work introduces a novel methodology for computing parameter gradients for any existing model-and-simulator combination, enabling both offline and online tuning, including the implementation of homeostatic-control mechanisms. Our approach seamlessly integrates traditional simulations with gradient-based optimization, facilitating scalable, robust and adaptive brain simulation without the need for developing new simulators.

Introduction

Building realistic models of the brain requires estimating many unobserved parameters because the complete dynamical-system state of the brain is not fully observable. It is due to this limitation that – despite nowadays being able to construct and simulate large brain models – they behave poorly once stretched beyond the specific problems for which they were designed. There are good reasons for this *parameter-tuning problem*: spatially detailed, biophysically realistic models contain a large number of parameters with nonlinear effects such as protein concentrations, synaptic connections or homeostatic dynamical behavior, all of which need to be constantly and concurrently tuned. Then, careful tuning of parameters is key to building robust, composable and adaptable brain models.

Tuning of these parameters can take place *offline*, externally to the simulator, or *online*, inside the simula-

tor, emulating biological *homeostatic control* [1]. General parameter-tuning methods can be divided into gradient-free or gradient-based ones. Gradients represent how changes in model parameters affect simulation output. Currently, gradient-free methods are the dominant approach for offline tuning of realistic brain models using existing brain simulations: manual parameter variation, evolutionary search or randomized search [2, 3, 4, 5]. However, these are known to suffer from the curse of dimensionality: higher-dimensional parameter spaces take exponentially longer to tune. Furthermore, they do not allow for tuning parameters during simulation, which at the moment requires carefully hand-crafted homeostatic control programs[1]. Instead, gradient-based methods do not suffer from this curse of dimensionality and scale to the tuning of billions of parameters, as exemplified by current large artificial intelligence models. What is more, online learning methods can also be developed based on gradients.

Unfortunately, existing brain simulators do not provide gradient calculation. The construction of new, gradient-enabled simulators from scratch is not a task to be taken up lightly. Maintaining feature compatibility and simulation consistency across simulators is heavily dependent on the simulator engine(s) selected and on the support of ecosystem software tools. There are currently two ongoing efforts building new simulators in an automatic-gradient environment [6, 7]. However, these simulators have still not reached NEURON-level compatibility and existing brain models are not supported in this format. Furthermore, they do not support online tuning, i.e., homeostatic control. In contrast, in this brief communication, we advocate for a methodology that enables the calculation of parameter gradients using *any unmodified*, existing model-and-neurosimulator combination and, subsequently, the support for homeostatic control.

Results

Let us assume a morphologically detailed, biophysically realistic model of a single neuron (fig. 1A-B). Within the brain-simulation software environment, a modeler essen-

arXiv:2412.07327v3 [q-bio.NC] 7 Jan 2025

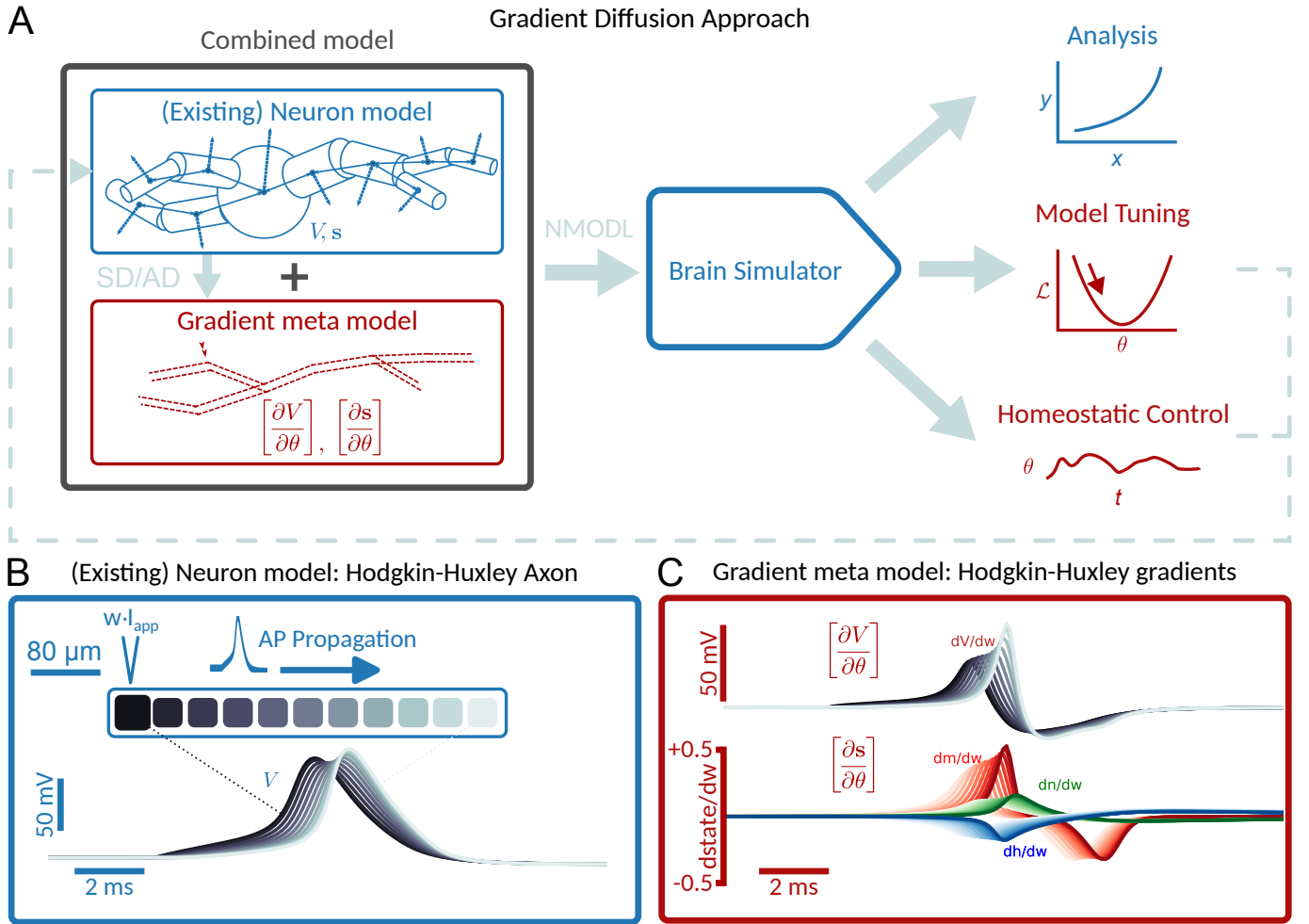


Figure 1: **A** Gradient-diffusion approach: A neuron model is enhanced with a gradient (meta) model, by symbolic or automatic differentiation. This creates a new model, which can be simulated by (existing) brain simulators. Resulting gradients can be used for tuning or homeostatic control, or be useful on their own. The neuron model is a discretized, multicompartmental, cable cell. Voltage diffusion happens along connected arrows, ion-channel/leak-based axial currents flow along dotted arrows. Mechanism state and voltages are maintained at filled circles. Such mechanisms, including both state derivatives and transmembrane currents, are written in NMODL files. **B** Hodgkin-Huxley (HH), linear axon model, with a pulse current applied on one end to create a propagating action potential (AP). Each compartment has a voltage, which is plotted, showing this propagation. **C** Gradient model of the HH model, showing the resulting gradients over time.

tially defines two sets of functions: The ion-channel current contribution i to the membrane potential V , and the time-derivative of the internal state variables \mathbf{s} . These functions are defined for each position on the spatial neuron and depend on a set of parameters θ :

$$i(V, \mathbf{s}, \theta) \quad (1)$$

$$\frac{d}{dt} \mathbf{s}(V, \mathbf{s}, \theta) \quad (2)$$

With this description in place, our goal is to find the gradients of the voltage V and state \mathbf{s} with respect to the parameters θ at any point in (simulation) time and for all compartments. To that end, we define a *gradient model* to be simulated alongside the neural model defined in eq. (1)

and eq. (2). This gradient model consists of the voltage gradients $\left[\frac{\partial V}{\partial \theta}\right]$ as diffusive ion-species and the state gradients $\left[\frac{\partial \mathbf{s}}{\partial \theta}\right]$ as internal state variables (fig. 1A-C). In our notation, brackets $([\cdot])$ denote new state variables introduced for the simulation of the gradient model. The gradient model calculates the voltage and state gradients via direct integration of the sensitivity equation (see Methods) by supplying the time derivatives of $\left[\frac{\partial V}{\partial \theta}\right]$ and $\left[\frac{\partial \mathbf{s}}{\partial \theta}\right]$ as mechanisms to the brain simulator:

$$\frac{d}{dt} \left[\frac{\partial V}{\partial \theta}\right] \left(V, \mathbf{s}, \theta, \left[\frac{\partial V}{\partial \theta}\right], \left[\frac{\partial \mathbf{s}}{\partial \theta}\right] \right) \quad (3)$$

$$\frac{d}{dt} \left[\frac{\partial \mathbf{s}}{\partial \theta}\right] \left(V, \mathbf{s}, \theta, \left[\frac{\partial V}{\partial \theta}\right], \left[\frac{\partial \mathbf{s}}{\partial \theta}\right] \right) \quad (4)$$

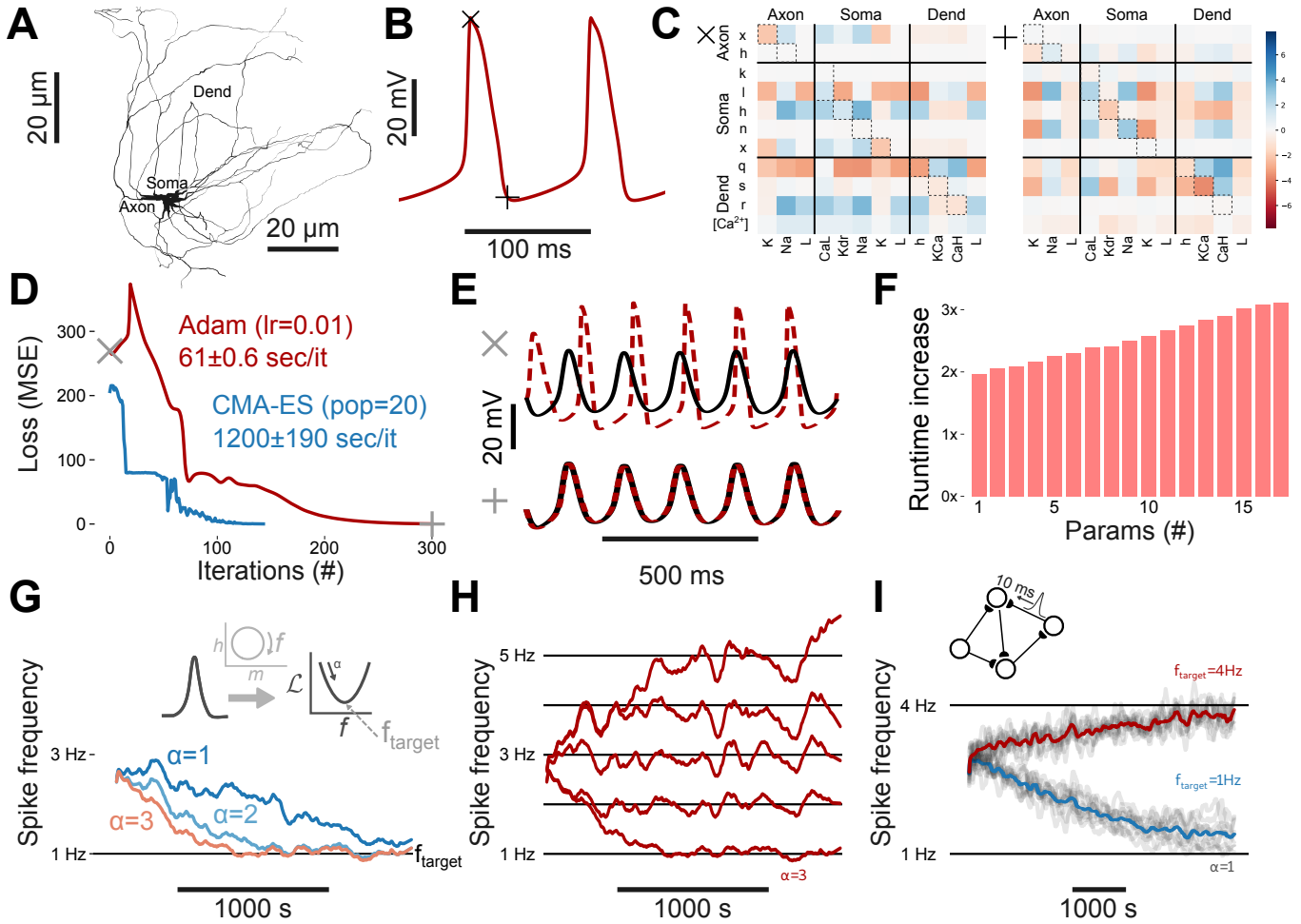


Figure 2: **A:** Simulated-neuron morphology **B:** Subthreshold Oscillation (STO) with specific timepoints (+ and ×) **C:** $\left[\frac{\partial s}{\partial \theta}\right]$ at specific timepoints from **B** **D:** Loss during optimization using gradient descent (Adam, red) and traditional evolutionary approach (CMA-ES, blue) **E:** Simulated (red) vs target (black) somatic membrane potential before (top) and after (bottom) training **F:** Increase in computational time relative to non-gradient simulation, when co-simulating the gradient model **G:** Homeostatic control of frequency via online learning. Frequency, in the Hodgkin-Huxley system, is derived from (m, h) -state trajectories (see Methods). Different traces show the effect of learning rate $(\alpha, \text{in } \cdot 10^{-6})$ on homeostatic control stability of frequency, with $\alpha > 3 \cdot 10^{-6}$ being unstable. The simulation is 2000 seconds, or 400 million time-steps in the Hodgkin-Huxley system. **H:** Homeostatic control with different target frequencies, same as **G**. **I:** Network tuning via homeostatic control. A network of 10 Hodgkin-Huxley neurons is simulated, where each neuron is receiving spike input from 3 other random neurons. While spike-gradients are not part of the gradient model, the system still tunes to the desired frequency.

These time derivatives can be obtained by either symbolic or automatic differentiation. Specifically, the gradient model can be fully expressed either as existing NMODL interfaces (fig. 3) or via the Arbor-PyCat interface developed in Methods, respectively.

Applications

We now demonstrate the application of gradients in brain models for tuning in the offline and online setting.

Gradient-Based Parameter Tuning Given a Loss function $\mathcal{L}(V, s)$, we can define gradient descent by integration over the total simulation time T as:

$$\theta \leftarrow \theta - \alpha \int_0^T \left(\frac{\partial \mathcal{L}}{\partial V} \left[\frac{\partial V}{\partial \theta} \right] + \frac{\partial \mathcal{L}}{\partial s} \left[\frac{\partial s}{\partial \theta} \right] \right) dt \quad (5)$$

Here, the application of gradients in brain simulation is external tuning of parameters. To show the applicability of the method, we developed the gradient-model of a 17-parameter Inferior Olivary Nucleus (ION) neuron model [7, 8] with experimentally obtained morphology (fig. 2A). These neurons express continuous subthreshold oscillations (fig. 2B). The gradients show how the interplay between parameters and state gives rises to the observed behaviour (fig. 2C). We optimized the aforementioned ION neuron model using gradient-descent [9, 10] to replicate a more

realistic sinusoidal, target-voltage trace. For comparison, traditional evolutionary search (CMA-ES [11]) was also included. Both optimization methods solve the problem successfully, but CMA-ES relies on more simulations per iteration, leading to ≈ 10 times longer optimization times (fig. 2D-E). Co-simulating a gradient system with the regular system for simulation increased simulation runtime by ≈ 2 times, after which, minor runtime increase per included parameter is observed fig. 2F.

Homeostatic Control The principal advantage of the co-simulated gradient model over externally calculated gradients, is access to gradients directly within the neural model. These can be used for *online* optimization of neurons; i.e., for emulating homeostatic control. This will allow us to tune whole networks of cells.

The goal of homeostatic control is to minimize an instantaneous error $e(V, \mathbf{s})$. For simplicity, we can assume that this error is a single element of \mathbf{s} , the integrated loss term $\mathbf{s}_0 = \int_0^t l(v, \mathbf{s})$ such that $e(V, \mathbf{s}) = \mathbf{s}_0$. Now, we can interpret gradient descent as an dynamical system with learning rate α :

$$\frac{d}{dt}\theta = -\alpha \frac{\partial e(\mathbf{s})}{\partial \mathbf{s}} \left[\frac{\partial \mathbf{s}}{\partial \theta} \right] + \xi \Delta_x \theta \quad (6)$$

The parameters are now diffusive ion species, where fast diffusion of gradient updates ξ enables non-local tuning. A gradient-forgetting parameter λ is not required to accommodate for the updated values of θ which are not reflected yet in $\left[\frac{\partial \mathbf{s}}{\partial \theta} \right]$ and to make sure the gradients do not explode for long running simulations. We denote these adjusted gradients with a prime ('):

$$\frac{d}{dt} \left[\frac{\partial a}{\partial \theta} \right]' = -\lambda \left[\frac{\partial a}{\partial \theta} \right]' + \frac{d}{dt} \left[\frac{\partial a}{\partial \theta} \right], \quad a \in \{V, \mathbf{s}\} \quad (7)$$

We applied homeostatic control to the Hodgkin-Huxley system, to tune the frequency of single neurons. Frequency was derived from the state dynamics (fig. 2G, top). Homeostatic control enables Hodgkin-Huxley neurons to tune, within a simulation, their frequency response to a varying noise input. Given appropriate balancing of α and λ , this leads to a stable system (see fig. 2G, Methods). The same method can be applied to tune for different target frequencies (fig. 2H). In the network setting, homeostatic tuning also stably enables frequency-tuning, although at a lower learning rate (fig. 2I).

Discussion

In this brief, we introduced *gradient diffusion*, a methodology that facilitates the calculation of parameter gradients for any existing, unmodified model-and-neurosimulator combination, thereby enabling support for homeostatic control. This approach allows for the efficient tuning of

realistic neuron models and the implementation of homeostatic mechanisms in large networks, with the overarching goal of developing more robust, composable, and adaptable brain models that elucidate both the slow and fast dynamics of the brain.

The fact that an unmodified simulator could be *tricked* into calculating gradients has broader implications across computational science. Many scientific disciplines use specialized simulation software for field-specific models. Due to the local nature of derivatives, gradient models share many characteristics with their source model. Similar tricks to gradient diffusion could thus be applied in different fields, leading to easier-to-tune models across scientific fields.

An interesting property of the gradient model is its representability as local dynamics and diffusive species. No nonphysical, non-local communication is required, which means that gradient calculating is reachable within biological constraints of cellular mechanisms. While cells are unlikely to keep track of an exact parameter-Jacobian, certain processes could be guided by cellular computed gradients.

A future research direction is deriving the brain's slow dynamics and learning mechanisms. Training many parameters over extended periods allows *black-box* models, such as neural networks representing protein networks, to act as homeostatic-control agents within cells. Promising results have emerged in simplified neuron models [12]. Transferring the approach to realistic neuron models creates a data-driven possibility to recover biological slow dynamics.

Limitations of the method relate to the fact that brain models extend beyond the cable equation: spike propagation with delays, stochastic models, reaction kinetics and ion dynamics, and Nernst potentials are not included in the method. These can be solved mathematically but would require modifications to the brain simulators, such as annotating spikes with gradient vectors. This omission does not directly affect homeostatic tuning: as shown, by handling some parameter-dependent processes as constant, networks can still be tuned. More complex tasks, like teaching a computational function to a network of cells, would require modification of existing simulators or development of a new, fully differentiable brain simulator.

Our methodology adopts forward propagation through time (FPTT), commonly employed in artificial-neural-network tuning. As demonstrated, this enables in-simulation parameter tuning and homeostatic control. Without the constraints imposed by transient-neurosimulator mechanics –characteristic of many simplified brain models – a range of alternatives, such as backward propagation through time, surrogate gradients, reverse-time adjoint-methods could be explored [13, 14]. However, implementing these would necessitate developing a novel neurosimulator from scratch. In this context, we are optimistic about the potential of future differentiable simulators, such as the ongoing Jaxley project [15].

Methods

In this section, we explain how the gradient model is derived from the cable equations and evaluate the approach. We start with a description of the cable equation as used in brain-simulation software, followed by a short description of the *sensitivity equation*. We then combine these equations to form the gradient model and discuss the stability of homeostatic mechanisms built on top of these gradients and the necessity of a forgetting parameter λ . We conclude with the evaluation methods.

Brain Simulation Computational neuroscience seeks to gain knowledge about the brain dynamics and function by simulation and analysis of biological models, at the required level of spatial and biophysical accuracy for the given research question.

The simplest possible equation to model a neuron at a biophysical level is the integration of current i over its capacitive membrane. This *transmembrane* current is usually the sum of individual modelled ionic-channel currents. The current through each ionic channel is calculated from the cell’s voltage, channel internal state \mathbf{s} and system parameters θ .

However, biological neurons, have an intricate spatial structure: Typically, a single root (soma), an axon and a branched dendritic tree. Modelling this accurately requires modelling the spatial structure of these neurons. In effect, beyond current influx and outflux over the capacitive (C_m) cell membrane, we also model the *longitudinal* current along the branches of the neural structure (fig. 1A, blue). This is visible as a diffusion operator (Δ_x/R_l) in the voltage equations.

In modelling, these spatial trees are discretized into *segments*, leading to *multicompartmental* neural models. Each segment is treated as a tapered cylinder. The longitudinal diffusion term takes this into account by considering the change in surface area with respect to longitudinal distance ($\frac{\partial S}{\partial x}$). Trivially, ($\frac{\partial S}{\partial x}$) = $2\pi R$ for a regular cylinder radius. Thus, we are left with the following *cable equation* [16, 17]

$$\frac{d}{dt}V = \frac{\Delta_x V}{C_m R_l \left(\frac{\partial S}{\partial x}\right)} - \frac{i(V, \mathbf{s}, \theta)}{C_m} \quad (8)$$

$$\frac{d}{dt}\mathbf{s} = \mathbf{f}(V, \mathbf{s}, \theta) \quad (9)$$

Brain-Simulation Software Biophysical realistic neurons are simulated using dedicated brain simulation platforms, including NEURON [18], Arbor [17], EDEN [19]. These contain the necessarily patchwork of mechanism to define a neural model. A full mathematical model describing these does not exist. Of great importance to the modeler is the interface used to describe the model to the simulator. NEURON and Arbor use the NMODL language to define mechanism dynamics, while EDEN is built around the NeuroML language. In Arbor, NMODL is compiled to a C++ *mechanism catalogue*, which then interfaces with

a common Application Binary Interface (ABI). The cable equation in eq. (8) is taken from the Arbor brain simulator, but the same equation is solved by NEURON or EDEN. On the programming side, these brain simulators allow the user to specify the functions $i(V, \mathbf{s}, \theta)$ and $\mathbf{f}(V, \mathbf{s}, \theta)$ using the NMODL or NeuroML languages, the rest is handled by the simulator.

Sensitivity Equation Assuming general dynamical system $\dot{x} = f(x, \theta)$, we have the time derivative of the state-parameter gradient as the sensitivity equation ([20]):

$$\frac{d}{dt} \left[\frac{\partial x}{\partial \theta} \right] = \frac{\partial f(x, \theta)}{\partial \theta} + \frac{\partial f(x, \theta)}{\partial x} \left[\frac{\partial x}{\partial \theta} \right] \quad (10)$$

where we denote with $\langle \cdot \rangle$ the state matrix of this new *gradient system*, for which we can explicitly solve using numerical integration.

Gradients for Brain Models The most obvious solution to calculate gradient for neural models is by automatic gradient calculation throughout the entire simulator [6, 15].

$$\frac{\partial V}{\partial \theta} = \frac{\partial}{\partial \theta} \text{ODESolve}(\dot{V}, \dot{\mathbf{s}}) \quad (11)$$

This does not work in practice, as automatic gradient calculation is not possible in any currently existing full-featured brain simulator. Writing an differentiable ODE-Solve function to handle brain models, would constitute to writing a new brain simulator from scratch, which is a long and costly effort. Instead, we implement a gradient simulators by co-simulating the *gradient model* of a neuron, in parallel to the neuron which is simulated by the simulator of choice. Our method leverages the development effort and optimization put into published complex simulations and enables computational neuroscientists to tackle new problems requiring on the fly gradient computation and optimization.

Applying the sensitivity equation eq. (10) to the cable equation eq. (8), we obtain the gradients for the cable cell. As such, we can now express a second *gradient model*, as:

$$\begin{aligned} \frac{d}{dt} \left[\frac{\partial V}{\partial \theta} \right] &= \frac{\Delta_x \left[\frac{\partial V}{\partial \theta} \right]}{C_m R_l \left(\frac{\partial S}{\partial x}\right)} - \frac{1}{C_m} \frac{\partial i}{\partial \theta} \\ &\quad - \frac{1}{C_m} \frac{\partial i}{\partial V} \left[\frac{\partial V}{\partial \theta} \right] - \frac{1}{C_m} \frac{\partial i}{\partial \mathbf{s}} \left[\frac{\partial \mathbf{s}}{\partial \theta} \right] \end{aligned} \quad (12)$$

$$\frac{d}{dt} \left[\frac{\partial \mathbf{s}}{\partial \theta} \right] = \frac{\partial \mathbf{f}}{\partial \theta} + \frac{\partial \mathbf{f}}{\partial V} \left[\frac{\partial V}{\partial \theta} \right] + \frac{\partial \mathbf{f}}{\partial \mathbf{s}} \left[\frac{\partial \mathbf{s}}{\partial \theta} \right] \quad (13)$$

Notably, the longitudinal voltage-diffusion term led to a *gradient-diffusion* term in the gradient model. Diffusion of state variables is not expressible in NEURON or Arbor. Instead, we can use built-in diffusion of custom ions, for example in Arbor [21]:

<pre> NEURON { SUFFIX gradient_model NONSPECIFIC_CURRENT i USEIONS x1..M WRITE xd1..M RANGE s, theta, [dV/dtheta], [ds/dtheta] } STATE { s ∈ ℝ^N [dV/dtheta] ∈ ℝ^M theta ∈ ℝ^M [ds/dtheta] ∈ ℝ^{N×M} } INITIAL { [ds/dtheta] = 0 [dV/dtheta] = 0 } </pre>	<pre> DERIVATIVE d { [dV/dtheta] = xd d/dt s = f(V, s, theta) d/dt [dV/dtheta] = -d/dt (di/Cm/dtheta) - d/dt (di/Cm/dV) [dV/dtheta] - d/dt (di/Cm/ds) [ds/dtheta] d/dt [ds/dtheta] = d/dt (df/dtheta) + d/dt (df/dV) [dV/dtheta] + d/dt (df/ds) [ds/dtheta] } BREAKPOINT { SOLVE d METHOD sparse i = i(V, s, theta) xd = [dV/dtheta] } </pre>
--	---

Figure 3: Implementation of the gradient model in the common NMODL interface. Right-hand side derivatives are to be calculated by symbolic or automatic gradient derivation. xd is a vector of ions. Some freedom of notation was allowed: NMODL does not support vectors or matrices. Instead, such objects should be read as written as single scalar values (i.e. $\mathbf{s} = s_1, s_2 \dots s_N$)

$$\frac{d}{dt}c = \frac{\beta \Delta_x}{\left(\frac{\partial S}{\partial x}\right)}c + i_c \quad (14)$$

by setting the ionic diffusivity $\beta = \frac{1}{C_m R_l}$ (in practice, $\beta = 100/C_m R_l$ after unit conversion). In this way, we can calculate gradients for multicompartmental cells against the normal Arbor user API.

The resulting gradient system reflects a lot about the underlying system. In the case of neurons, we can express the gradient system as a ion-channel mechanism and a set of extra diffusive ions. Their dynamics can be derived by (automatic) gradient calculation from the existing neuron model. A template NMODL file implementing the gradient model is shown in fig. 3.

Homeostatic-Control Stability Consider a passive neuron model with a target potential and leak, reversal potential as parameter:

$$i = g_{\text{leak}}(V - E_{\text{leak}}) \quad \frac{d}{dt}\mathbf{s} = \frac{1}{2}(V - E_{\text{target}})^2 \quad (15)$$

$$\theta = E_{\text{leak}} \quad e = s_0 \quad (16)$$

which leads to the following nonlinear system of PDEs for a single linear neuron with no varying radius, where we have included a gradient-forgetting parameter λ from eq. (7) to prevent stability problems (as will be shown next):

$$\frac{d}{dt}V = \frac{\Delta_x V}{2\pi R C_m R_l} - \frac{g_{\text{leak}}(V - E_{\text{leak}})}{C_m} \quad (17)$$

$$\frac{d}{dt}\left[\frac{\partial V}{\partial \theta}\right] = \frac{\Delta_x \left[\frac{\partial V}{\partial \theta}\right]}{2\pi R C_m R_l} + \frac{g_{\text{leak}}}{C_m} \left(1 - \left[\frac{\partial V}{\partial \theta}\right]\right) \quad (18)$$

$$\frac{d}{dt}\theta = -\alpha \left[\frac{\partial \mathbf{s}}{\partial \theta}\right] \quad (19)$$

$$\frac{d}{dt}\left[\frac{\partial \mathbf{s}}{\partial \theta}\right]' = -\lambda \left[\frac{\partial \mathbf{s}}{\partial \theta}\right]' + (V - E_{\text{target}}) \left[\frac{\partial V}{\partial \theta}\right] \quad (20)$$

After the initial transient we obtain $\left[\frac{\partial V}{\partial \theta}\right] = 1$. Without loss of generality, we can set $E_{\text{target}} = 0$. If we now apply a spatial sinusoidal perturbation $V \propto \sin(\omega x)$, we obtain the linear system:

$$\frac{d}{dt} \begin{pmatrix} V \\ \left[\frac{\partial \mathbf{s}}{\partial \theta}\right]' \\ E_{\text{leak}} \end{pmatrix} = \begin{pmatrix} \frac{-g_{\text{leak}}}{C_m} - \frac{\omega^2}{2\pi R C_m R_l} & 0 & \frac{g_{\text{leak}}}{C_m} \\ 1 & -\lambda & 0 \\ 0 & -\alpha & 0 \end{pmatrix} \begin{pmatrix} V \\ \left[\frac{\partial \mathbf{s}}{\partial \theta}\right]' \\ E_{\text{leak}} \end{pmatrix} \quad (21)$$

and resulting Routh-Hurwitz stability criterion[22]:

$$\alpha < \frac{(\pi C_m^2 R R_l \text{leak} \lambda \omega^2 + 2g_{\text{leak}} \lambda) (\pi C_m^2 R R_l \omega^2 + 2C_m \lambda + 2g_{\text{leak}})}{4C_m g_l} \quad (22)$$

which has a lower bound as $\alpha < \lambda \left(\lambda + \frac{g_l}{C_m}\right)$ in the case $\omega = 0$ (or a single point neuron). In other words: to

have stable online learning, the gradient needs to forget. Beyond this, spatial perturbations do not make the system more unstable. The same analysis can be repeated by adding a $\beta_\theta \Delta_x \theta$ diffusion term to the theta equation, where again spatial perturbations do not lead to a more unstable system.

Arbor-Pycat Library Crucial in the method is availability of gradients for the current and ode system, greatly amplified by automatic gradients calculation systems - eg. JAX. JAX, as an ML-library, fully expresses the desired interface for expressing internal dynamics of neural models [23]. To ease implementation, a python wrapper around the C mechanism ABI was written that exposed the mechanism internals as numpy-style buffers, allowing JAX to work with it. This is released as a installable python package *Arbor-Pycat* [24].

Axon model The Hodgkin-Huxley model was implemented in Arbor-Pycat, as well as its gradient system using eq. (13). An axon was defined of 11 compartments, using the resulting mechanism. A current pulse was applied at $t=200\text{ms}$ and multiplied by the parameter $\theta = w$ before being injected into one end of the axon.

Inferior Olivary Nucleus model A modified version [8] of the de Gruijl model [7] was implemented in Arbor-Pycat. The morphology of mouse IO neuron C4A was used [25]. After discretization, it contains 4 axonal, 15 dendritic and 2 somatic compartments. Initial parameters are listed in Table 1. For programming ease, these default values were scaled by the parameter θ , which was thus a vector of ones, initially. Optimization was performed against the loss-function:

$$\mathcal{L} = \frac{1}{T} \int_0^T (v(t) - \hat{v}(t))^2 dt \quad (23)$$

from which updates to the state were calculated from eq. (5). The Adam optimizer [9] with learning rate 10^{-2} was used, via the optax library [10]. This was compared to the the CMA-ES[11] algorithm with population size 20 and initial $\sigma = 0.1$. Initial parameters are listed in table 1.

Homeostatic control of spike frequency Experiments on the usability of gradients for homeostatic control were performed in the Hodgkin-Huxley model. The target was a given spiking frequency, while a Ornstein-Uhlenback noise input was given as current input. Tunable parameters were the conductance values of the sodium and potassium channels, and the input scaling. To also show the usability of the method through standard NMODL interface, the Hodgkin-Huxley model was implemented symbolically in SymPy. The SymPy library was then used to implement the gradient model in NMODL code.

The online frequency-tuning task requires a differentiable measure of spike frequency that is calculable from

Soma (S/cm ²)	Dendrite (S/cm ²)
$g_{\text{leak}} = 1.3 \times 10^{-5}$	$g_{\text{leak}} = 1.3 \times 10^{-5}$
$g_{\text{CaL}} = 0.045$	$g_{\text{KCa}} = 0.220$
$g_{\text{Na}} = 0.030$	$g_{\text{CaH}} = 0.010$
$g_{\text{Kdr}} = 0.030$	$g_{\text{h}} = 0.015$
$g_{\text{K}} = 0.015$	
Axon (S/cm ²)	Potential (mV)
$g_{\text{leak}} = 1.3 \times 10^{-5}$	$V_{\text{leak}} = 10$
$g_{\text{Na}} = 0.200$	$V_{\text{Ca}} = 120$
$g_{\text{K}} = 0.200$	$V_{\text{Na}} = 55$
	$V_{\text{K}} = -75$
	$V_{\text{h}} = -43$

Table 1: Initial parameters for inferior olivary cell model

the cell state. For the Hodgkin-Huxley system, this cell state are the gating variables $\mathbf{s} = (m, h, n)$. We hypothesized that a robust metric could be the amount of revolutions in the gating-variable phase plane. Preliminary visual inspection suggested (m, \dot{m}) to be one of the more optimal choices, but the extra time dependence \dot{m} would add a lot of compute. Instead, it was decided to count the amount of revolutions in the (m, h) phase plane:

$$N = \frac{1}{2\pi} \text{unwrap} \left(\arctan2 \left(m - \frac{1}{2}, h - \frac{1}{2} \right) \right) \quad (24)$$

which derivative (eq. (25)) is low-passed (eq. (26)) to obtain a differentiable frequency metric. The final instantaneous error-function is then the squared difference to the target frequency (eq. (27)):

$$\frac{d}{dt} N = \frac{1}{2\pi} \frac{(h - \frac{1}{2}) \frac{d}{dt} m - (m - \frac{1}{2}) \frac{d}{dt} h}{(h - \frac{1}{2})^2 + (m - \frac{1}{2})^2} \quad (25)$$

$$\tau_f \frac{d}{dt} f = \frac{d}{dt} N - f \quad (26)$$

$$\frac{d}{dt} e = \frac{1}{2} (f - f_{\text{tgt}})^2 \quad (27)$$

Here, τ_f is preferable on a time scale much larger than the expected spiking frequency (e.g. $\tau_f \approx 10/f_{\text{tgt}}$)

Hardware AMD Ryzen 9 3900X 12-Core processor and NVIDIA RTX 6000 GPU

Acknowledgments This paper is partially supported by the European-Union Horizon Europe R&I program through projects SEPTON (no. 101094901) and SECURED (no. 101095717) and through the NWO - Gravitation Programme DBI2 (no. 024.005.022). The RTX6000 used for this research was donated by the NVIDIA Corporation.

References

- [1] Timothy O’Leary, Alex H Williams, Alessio Franci, and Eve Marder. Cell types, network homeostasis, and pathological compensation from a biologically plausible ion channel expression model. *Neuron*, 82(4):809–821, 2014.
- [2] Quentin JM Huys, Misha B Ahrens, and Liam Paninski. Efficient estimation of detailed single-neuron models. *Journal of neurophysiology*, 96(2):872–890, 2006.
- [3] Willem AM Wybo, Jakob Jordan, Benjamin Ellenberger, Ulisses Marti Mengual, Thomas Nevian, and Walter Senn. Data-driven reduction of dendritic morphologies with preserved dendro-somatic responses. *Elife*, 10:e60936, 2021.
- [4] Werner Van Geit, Michael Gevaert, Giuseppe Chindemi, Christian Rössert, Jean-Denis Courcol, Eilif Benjamin Muller, Felix Schürmann, Idan Segev, and Henry Markram. Bluepyopt: Leveraging open source software and cloud infrastructure to optimise model parameters in neuroscience. *Frontiers in Neuroinformatics*, 10(17), 2016. ISSN 1662-5196. doi: 10.3389/fninf.2016.00017.
- [5] Pedro J Gonçalves, Jan-Matthis Lueckmann, Michael Deistler, Marcel Nonnenmacher, Kaan Öcal, Giacomo Bassetto, Chaitanya Chintaluri, William F Podlaski, Sara A Haddad, Tim P Vogels, et al. Training deep neural density estimators to identify mechanistic models of neural dynamics. *Elife*, 9:e56261, 2020.
- [6] Ilenna Simone Jones and Konrad Paul Kording. Efficient optimization of ode neuron models using gradient descent. *arXiv preprint arXiv:2407.04025*, 2024.
- [7] Jornt R De Gruijl, Paolo Bazzigaluppi, Marcel TG de Jeu, and Chris I De Zeeuw. Climbing fiber burst size and olivary sub-threshold oscillations in a network setting. *PLoS computational biology*, 8(12): e1002814, 2012.
- [8] Mario Negrello, Pascal Warnaar, Vincenzo Romano, Cullen B Owens, Sander Lindeman, Elisabetta Iavarone, Jochen K Spanke, Laurens WJ Bosman, and Chris I De Zeeuw. Quasiperiodic rhythms of the inferior olive. *PLoS computational biology*, 15(5): e1006475, 2019.
- [9] Diederik P Kingma. Adam: A method for stochastic optimization. *arXiv preprint arXiv:1412.6980*, 2014.
- [10] DeepMind, Igor Babuschkin, Kate Baumli, Alison Bell, Surya Bhupatiraju, Jake Bruce, Peter Buchlovsky, David Budden, Trevor Cai, Aidan Clark, Ivo Danihelka, Antoine Dedieu, Claudio Fantacci, Jonathan Godwin, Chris Jones, Ross Hemsley, Tom Hennigan, Matteo Hessel, Shaobo Hou, Steven Kapurowski, Thomas Keck, Iurii Kemaev, Michael King, Markus Kunesch, Lena Martens, Hamza Merzic, Vladimir Mikulik, Tamara Norman, George Papanikarior, John Quan, Roman Ring, Francisco Ruiz, Alvaro Sanchez, Laurent Sartran, Rosalia Schneider, Eren Sezener, Stephen Spencer, Srivatsan Srinivasan, Miloš Stanojević, Wojciech Stokowiec, Luyu Wang, Guangyao Zhou, and Fabio Viola. The DeepMind JAX Ecosystem, 2020. URL <http://github.com/google-deepmind>.
- [11] Nikolaus Hansen, Youhei Akimoto, and Petr Baudis. CMA-ES/pycma on Github. Zenodo, DOI:10.5281/zenodo.2559634, February 2019. URL <https://doi.org/10.5281/zenodo.2559634>.
- [12] Elias Najarro and Sebastian Risi. Meta-learning through hebbian plasticity in random networks. *Advances in Neural Information Processing Systems*, 33: 20719–20731, 2020.
- [13] Emre O Neftci, Hesham Mostafa, and Friedemann Zenke. Surrogate gradient learning in spiking neural networks: Bringing the power of gradient-based optimization to spiking neural networks. *IEEE Signal Processing Magazine*, 36(6):51–63, 2019.
- [14] Patrick Kidger. On neural differential equations. *arXiv preprint arXiv:2202.02435*, 2022.
- [15] Michael Deistler, Kyra L. Kadhim, Matthijs Pals, Jonas Beck, Ziwei Huang, Manuel Gloeckler, Janne K. Lappalainen, Cornelius Schröder, Philipp Berens, Pedro J. Gonçalves, and Jakob H. Macke. Differentiable simulation enables large-scale training of detailed biophysical models of neural dynamics. *bioRxiv*, 2024. doi: 10.1101/2024.08.21.608979.
- [16] Michael L Hines and Nicholas T Carnevale. The neuron simulation environment. *Neural computation*, 9(6):1179–1209, 1997.
- [17] N. Abi Akar, B. Cumming, V. Karakasis, A. Küsters, W. Klijn, A. Peyser, and S. Yates. Arbor — A Morphologically-Detailed Neural Network Simulation Library for Contemporary High-Performance Computing Architectures. In *2019 27th Euromicro International Conference on Parallel, Distributed and Network-Based Processing (PDP)*, pages 274–282, feb 2019. doi: 10.1109/EMPDP.2019.8671560.
- [18] Nicholas T Carnevale and Michael L Hines. *The NEURON book*. Cambridge University Press, 2006.
- [19] Sotirios Panagiotou, Harry Sidiropoulos, Dimitrios Soudris, Mario Negrello, and Christos Strydis. Eden: A high-performance, general-purpose, neuroml-based neural simulator. *Frontiers in neuroinformatics*, 16: 724336, 2022.

- [20] Thomas Hakon Gronwall. Note on the derivatives with respect to a parameter of the solutions of a system of differential equations. *Annals of Mathematics*, 20(4):292–296, 1919.
- [21] Nora Abi Akar, John Biddiscombe, Benjamin Cumming, Marko Kabic, Vasileios Karakasis, Wouter Klijn, Anne Küsters, Alexander Peyser, Stuart Yates, Thorsten Hater, Brent Huisman, Espen Hagen, Robin De Schepper, Charl Linssen, Harmen Stoppeles, Sebastian Schmitt, Felix Huber, Max Engelen, Fabian Bösch, Jannik Luboeinski, Simon Frasch, Lukas Drescher, and Lennart Landsmeer. Arbor library v0.9.0, November 2023. URL <https://doi.org/10.5281/zenodo.8233847>.
- [22] Carl Sandrock. tbcontrol: A python library for textbook control problems. URL <https://github.com/alchemyst/Dynamics-and-Control>.
- [23] Lennart PL Landsmeer, Max CW Engelen, Rene Miedema, and Christos Strydis. Tricking ai chips into simulating the human brain: A detailed performance analysis. *Neurocomputing*, page 127953, 2024.
- [24] Lennart Landsmeer. arbor-pycat, December 2024. URL <http://dx.doi.org/10.5281/zenodo.14506753>.
- [25] Nora Vrieler, Sebastian Loyola, Yasmin Yarden-Rabinowitz, Jesse Hoogendorp, Nikolay Medvedev, Tycho M Hoogland, Chris I De Zeeuw, Erik De Schutter, Yosef Yarom, Mario Negrello, et al. Variability and directionality of inferior olive neuron dendrites revealed by detailed 3d characterization of an extensive morphological library. *Brain Structure and Function*, 224(4):1677–1695, 2019.